ELSEVIER

Biochimica et Biophysica Acta 1328 (1997) 125–139

BIOCHIMICA ET BIOPHYSICA ACTA
BBA

Amphipathic peptide affects the lateral domain organization of lipid bilayers

I.V. Polozov [a], A.I. Polozova [a], J.G. Molotkovsky [b], R.M. Epand [a,*]

[a] *Department of Biochemistry, McMaster University, 1200 Main St. West, Hamilton, Ont. L8N 3Z5 Canada*
[b] *M.M. Shemyakin Institute of Bioorganic Chemistry, Russian Academy of Sciences, Moscow 117871, Russia*

Received 15 January 1997; revised 3 April 1997; accepted 10 April 1997

Abstract

Using lipid-specific fluorescent probes, we studied the effects of amphipathic helical, membrane active peptides of the A- and L-type on membrane domain organization. In zwitterionic binary systems composed of mixtures of phosphatidylcholine and phosphatidylethanolamine, both types of peptides associated with the fluid phase. While binding with high affinity to fluid membranes, peptides were unable to penetrate into the lipid membrane in the gel state. If trapped kinetically by cooling from the fluid phase, peptides dissociated from the gel membrane on the time scale of several hours. While the geometrical shape of the α-helical peptides determines their interactions with membranes with non-bilayer phase propensity, the shape complementarity mechanism by itself is unable to induce lateral phase separation in a fluid membrane. Charge–charge interactions are capable of inducing lateral domain formation in fluid membranes. Both peptides had affinity for anionic lipids which resulted in about 30% enrichment of acidic lipids within several nanometers of the peptide's tryptophan, but there was no long-range order in peptide-induced lipid demixing. Peptide insertion in fluid acidic membranes was accompanied by only a small increase in bilayer surface and a decrease in polarity in the membrane core. Peptide–lipid charge–charge interactions were also capable of modulating existing domain composition in the course of the main phase transition in mixtures of anionic phosphatidylglycerol with zwitterionic phosphatidylcholine. © 1997 Elsevier Science B.V.

Keywords: Fluorescence; Lipid specific probe; Membrane; Segregation

Abbreviations: DOPC, 1,2-dioleoyl-*sn*-glycero-3-phosphocholine; DMPC, 1,2-dimyristoyl-*sn*-glycero-3-phosphocholine; DPPC, 1,2-dipalmitoyl-*sn*-glycero-3-phosphocholine; DOPE, 1,2-dioleoyl-*sn*-glycero-3-phosphoethanolamine; DMPE, 1,2-dimyristoyl-*sn*-glycero-3-phosphoethanolamine; DMPG, 1,2-dimyristoyl-*sn*-glycero-3-phosphoglycerol; DPPG, 1,2-dipalmitoyl-*sn*-glycero-3-phosphoglycerol; DOPG, 1,2-dioleoyl-*sn*-glycero-3-phosphoglycerol; APC, 1-acyl-2-[*trans*-12-(9-anthryl)-11-dodecenoyl]-*sn*-glycero-3-phosphocholine; APE, 1-acyl-2-[*trans*-12-(9-anthryl)-11-dodecenoyl]-*sn*-glycero-3-phosphoethanolamine; APG, 1-acyl-2-[*trans*-12-(9-anthryl)-11-dodecenoyl]-*sn*-glycero-3-phosphoglycerol; APL, anthrylvinyl-labeled phospholipid (any of APC, APE or APG); PPC, 1-acyl-2-[9-(3-perylenoyl)nonanoyl]-*sn*-3-glycerophosphocholine; 18L, GIKKFLGSIWKFIKAFVG; Ac-18A-NH_2, *N*-acetyl-DWLKAFYDKVAEKLKEAF-amide; MLV, multilamellar vesicles; LUV, large unilamellar vesicles; FRET, fluorescence resonance energy transfer; *E*, fluorescence resonance energy transfer efficiency

* Corresponding author. E-mail: Epand@fhs.csu.mcmaster.ca

PII S0005-2736(97)00080-1

1. Introduction

There have been many studies on the lipid domain organization of biological membranes and there is accumulating evidence of its biological importance [1–3]. The domains arise over a large range of time- and length-scales, from dynamic organization on the nanometer scale [4,5] to the domains of micron scale, presenting fractions of the entire cell surface [6]. However, the factors inducing such an organization are not yet completely understood. It is often supposed that lateral organization can be induced by membrane proteins or peptides. The greatest attention has been drawn to the possibility of domain formation by transmembrane hydrophobic α-helical segments via the hydrophobic mismatch mechanism [7,8]. Less is known about peptides inserting parallel to the surface of the membrane which is often the case for amphipathic α-helical peptides, that is peptides which can potentially form a helix with opposing hydrophilic and hydrophobic faces oriented along its long axis. This structural feature is widely found in naturally occurring protein and peptides sequences [9]. In this paper, we report the effects on the membrane lateral organization of two amphipathic peptides, 18L and Ac-18A-NH_2, which feature the archetype sequences of the L- and A-type amphipathic α-helix according to a classification [10] based on the size and charge distribution of peptide hydrophilic domains. Because of their effect on the L_α–H_{II} phase transition, Ac-18A-NH_2 and 18L have been designated as bilayer stabilizer and destabilizer, respectively. This property is attributed to the difference in the geometric shapes of peptide molecules, that is, to the difference in the membrane location and size of the hydrophilic and hydrophobic domains in the membrane-active α-helical conformation [11]. 18L has a narrow, positively charged hydrophilic region and a large hydrophobic volume, contrary to Ac-18A-NH_2 with a narrower hydrophobic region and a wide surface of positively and negatively charged amino acid residues. Ac-18A-NH_2 and 18L peptides were shown to associate with membranes as monomers, presumably in the α-helical conformation parallel to the surface of the membrane [11–13], at least at low peptide–lipid molar ratios. Activities of these peptides are affected by membrane composition, namely by the presence of acidic or non-bilayer forming lipids. While acidic lipids similarly increase activities of both peptides, the presence of non-bilayer forming lipids enhances the lytic activities of 18L and decreases those of Ac-18A-NH_2 [12]. These properties, taken together with high membrane affinity, make these peptides an interesting choice for examining general peptide effects on the lateral organization of lipid membranes.

The use of semi-synthetic phospholipids carrying a fluorophore at the end of one of the hydrocarbon chains is becoming increasingly popular for studies of membrane structure and dynamics [14,32]. If the fluorophore is non-polar and not bulky, such probes may be expected to behave in multicomponent systems similar to their unlabeled counterparts. The 9-anthrylvinyl fluorophore (AV) has been found to conform to these requirements. AV has an excitation maximum at 360 nm which makes it possible for use as a resonance energy transfer acceptor from tryptophan. Its fluorescence lifetime of ~ 9 ns makes the fluorescence anisotropy of this probe sensitive to the phase state of the lipid [15,16]. Perylenoyl-labeled lipids had been synthesized as an acceptor for the anthrylvinyl excitation energy [17]. Perylenoyl fluorescence was found to be sensitive to the polarity of the environment and this was used to estimate the penetration of water into the lipid bilayer [18]. Taken together, these two lines of lipid-specific probes are very suitable for the studies of lipid–lipid and peptide–lipid interactions.

In this paper, using anthrylvinyl- and perylenoyl-labeled lipid-specific fluorescent probes, we studied the effects of the membrane active peptides, Ac-18A-NH_2 and 18L, on the lateral segregation of lipids in model binary lipid systems. We found that charge–charge interactions between the peptide and the lipid were capable of inducing lateral separation of lipid components. The geometric shape compensation mechanism on its own was unable to explain domain formation. We studied peptide effects on lipid mixing in a miscible fluid phase as well as peptide effects on pre-existing domain structure and peptide effects on the gel-to-liquid phase transition. In zwitterionic membranes, both types of peptides tended to partition into the fluid phase rather than the gel phase. However, these peptides could be kinetically trapped in the gel phase, dissociating on a time scale of hours. When the membranes contained acidic lipids, associa-

tion of both types of peptides with acidic lipids was stronger than the peptide preference for the fluid phase. That is, peptides preferentially partitioned into either the gel or fluid phase, depending on whether the acidic lipid-rich component was the high or low melting one. As determined from fluorescence energy transfer, peptide incorporation into the fluid phase was accompanied by little surface area increase, but was accompanied by an increase in the hydrophobicity of the membrane interior. We discuss peptide effects on lateral membrane organization in the general context of peptide membrane interactions.

2. Materials and methods

2.1. Materials

DOPC, DMPC, DPPC, DOPE, DMPE, DMPG, and DPPG were purchased from Avanti Polar Lipids (Alabaster, AL) and were used without further purification. 1-Acyl-2-[*trans*-12-(9-anthryl)-11-dodecenoyl]-*sn*-glycero-3-phosphocholine (APC), 1-acyl-2-[*trans*-12-(9-anthryl)-11-dodecenoyl]-*sn*-glycero-3-phosphoethanolamine (APE), 1-acyl-2-[*trans*-12-(9-anthryl)-11-dodecenoyl]-*sn*-glycero-3-phosphoglycerol (APG) and 1-acyl-2-[9-(3-perylenoyl)nonanoyl]-*sn*-glycero-3-phosphocholine (PPC) were synthesized as previously reported [19–22]. Details of the synthesis and characterization of the peptides have been described elsewhere [11,13]. The following peptides were used in the work: 18L, GIKKFLGSIWKFIKAFVG [11]; Ac-18A-NH_2, *N*-acetyl-DWLKAFYDKVAEKLKEAF-amide (see [13]). All other reagents were of analytical grade. Buffers were prepared in double-distilled deionized water.

2.2. Liposome preparation

Multilamellar vesicles (MLV) were made from vacuum-dried lipid films by suspending them in an appropriate buffer (20 mM Tris-HCl, 1 mM EDTA, 0.02% NaN_3, pH 7.4, unless otherwise stated) at a temperature at least 10EC above the temperature of the main phase transition of the corresponding lipid, followed by shaking and less than 20 seconds of low power sonication. Large unilamellar vesicles (LUV) were made by multiple extrusion of MLV through two stacked 100-nm pore polycarbonate filters (Nucleopore Corp., Pleasanton, CA). Lipid concentration was determined using a phosphate assay [23]. For experiments with MLV (anisotropy), to ensure equilibration between various lipid bilayers, peptides were added to the lipid solution in chloroform/methanol, before solvent evaporation. In LUV experiments, peptide addition to vesicle suspensions was accompanied with vigorous mixing to ensure equilibrium peptide distribution among vesicles.

Since many properties of lipid membranes are history dependent, a standard procedure was used for temperature-scanning experiments. Unless otherwise stated, before data acquisition, vesicles were cycled through the phase transition and kept at 4°C for 30 min, prior to use. Heating was usually performed at 0.5°C/min. Cooling was performed at the same rate immediately after completion of the heating scan.

2.3. Fluorescence measurements

Fluorescence experiments were done on an SLM AB-2 fluorometer (Urbana, IL). Unless otherwise stated, measurements were done in thermostated 3-ml quartz cuvettes with stirring at a lipid concentration of 100 μM. The temperature of the sample was usually monitored by a thermistor probe inserted in the cuvette.

Anisotropy of the fluorescence of the APC, APE and APG probes was measured in the L-format with excitation at 365 nm and emission at 435 nm. Cut-off filters have been placed in both the excitation and the emission paths to reduce light-scattering artifacts. The positions of the polarizers were changed automatically using the AB-2 SLM Aminco software. MLVs labeled with 0.2% of the anthrylvinyl probe were used for anisotropy measurements.

Tryptophan fluorescence emission spectra were recorded in the range from 310 to 480 nm, using an excitation wavelength of 280 nm. Anthrylvinyl fluorescence was excited at 365 nm and recorded from 390 to 480 nm. Perylenoyl fluorescence was excited at 435 nm and recorded from 470 to 600 nm. Background was routinely subtracted. A more complex correction of spectra was unnecessary since the lipid concentrations used in the experiments were below 0.2 mM in order to reduce scattering artifacts.

Fluorescence resonance energy transfer (FRET)

from peptide tryptophan to the anthrylvinyl probe (APC, APE, or APG) was monitored either by measuring the fluorescence intensity with the excitation at 280 nm and emission at 435 nm, using 4 nm monochromator slits, or was calculated from consecutive fluorescence emission spectra recorded in the range from 310 nm to 480 nm also using excitation at 280 nm.

Fluorescence resonance energy transfer from the anthrylvinyl probe to the perylenoyl probe was monitored either by measuring fluorescence intensities with excitation at 365 nm and emission at 510 nm and 435 nm using 4-nm monochromator slits or was calculated from fluorescence emission spectra recorded in the range from 390 to 600 nm using 365 nm excitation. Background due to scattering and emission resulting from direct excitation of the perylenoyl probe were routinely subtracted. Vesicles were labeled with 2 molar % of the anthrylvinyl probe and 1 molar % of the perylenoyl probe.

2.4. FRET efficiency calculations

The conventional method of presenting data on fluorescence resonance energy transfer is via calculating the transfer efficiency (E). According to Lakowicz [24], $E=(I_o-I)/I_o$, where I_o is the fluorescence intensity of donor in the absence of acceptor and I is the intensity in the presence of acceptor. This formula can be applied directly, if it is possible to measure the fluorescence intensity of the donor in the absence of the acceptor. This approach was used for the calculation of the efficiency of FRET from anthrylvinyl- to perylenoyl-labeled phospholipid in the peptide titration experiments. To eliminate FRET, we added the detergent Triton X-100 to dilute the phospholipids. Control experiments show that solubilization with Triton X-100 does not significantly change the integral intensity of the unquenched anthrylvinyl-labeled fluorophore. Intensity was usually measured within the range of 400–450 nm.

The approach described above was not suitable for the studies of FRET from peptide tryptophan to the anthrylvinyl probe (APC, APE, or APG) as tryptophan fluorescence is more sensitive to the polarity of the environment and also at 280 nm, commercially available detergents have a high background fluorescence and/or absorption. To calculate fluorescence resonance energy transfer efficiency from the peptide to the anthrylvinyl probe, the fluorescence emission spectra were fitted with the sum of peptide and probe fluorescence components. The transfer efficiency was then calculated as $E=(I_a/Q_a)/(I_t+I_a/Q_a)$, where I_a is the integral intensity of anthrylvinyl fluorescence, Q_a is the quantum yield of anthrylvinyl fluorescence and I_t is the integral intensity of peptide fluorescence. The quantum yield of anthrylvinyl fluorescence is ~ 0.59 as previously reported [25].

The temperature dependence of peptide induced lateral organization was calculated from the efficiency of APL/PPC FRET in the experiments which simultaneously monitored the intensities of fluorescence at 435 and 510 nm using 365 nm excitation. Efficiency was determined as $E=(I_p/Q_p)/(I_a+I_p/Q_p)$, where I_a is the intensity of anthrylvinyl fluorescence (435 nm), Q_p is the quantum yield of perylenoyl fluorescence (~ 0.65, according to Molotkovsky et al. [17]), and I_p is the intensity of perylenoyl fluorescence (510 nm).

2.5. Surface area increase

As had been shown by Fung and Stryer [26], in the case of randomly distributed donor and acceptor in one plane, FRET efficiency is defined as:

$$E=1-\frac{1}{\tau_o}\cdot\int_0 \exp\left(\frac{-t}{\tau_o}\right)\cdot\exp\left(-\sigma_a\int_a \times\left[1-\exp\left(-\left(\frac{t}{\tau_o}\right)\left(\frac{R_o}{r}\right)\right)^6\right]2\pi r dr\right)dt$$

where R_o is the Foerster radius for the donor/acceptor pair, σ_a is the surface density of the acceptor, τ_o is the fluorescence lifetime of the donor in the absence of the acceptor. The second exponent in the equation is the energy transfer term. Integration is performed over the whole range of possible distances between donor and acceptor (r), starting with a the distance of the closest approach of the donor and acceptor. Efficiency is independent of the surface density of the donor, and it is not very sensitive to a. Quantitative integration [26] shows that for a Foerster radius (R_o) within 20–60 Å, up to $E\sim 0.4$, the efficiency is approximately proportional to the sur-

face density of the acceptor (σ_a), that is $E\ \sigma_a$. This also can be shown more rigorously. Taking into account following relationships:

$$\sigma_a = (n_a/n_l)/s_l \quad \Delta S = s_p \times p \quad S_o = s_l \times l$$

where s_l is the surface area of one lipid molecule, s_p is the surface increase due to membrane incorporation of one peptide molecule, n_a/n_l is the molar fraction of acceptor molecules in the membrane, ΔS is the change in membrane surface (S_o), p is peptide concentration, l is lipid concentration, ΔE is the change in FRET efficiency (E_o). We have at linear approximation:

$$\Delta E/E_o = -\Delta S/S_o = -s_p/s_l \times p/l$$

that is, the slope of the initial linear part of the plot of $\Delta E/E_o$ vs. p/l will give the ratio of the surface increase due to one peptide compared to that produced by one lipid molecule.

3. Results

3.1. Metastability of peptide association with gel state membranes

In water, the 18L and Ac-18A-NH_2 peptides exist as monomers [12]. Binding of peptides to membranes has been characterized from a blue shift of tryptophan fluorescence emission. The model of dynamic membrane partitioning of monomers successfully described both the equilibrium and kinetics of peptide membrane binding. For fluid lipid membranes, binding constants of Ac-18A-NH_2 and 18L were within 10^4–10^7 M^{-1} [12]. Knowledge of binding constants makes it possible to choose experimental conditions such that the peptide is essentially all bound to the membrane and thus the total peptide/lipid ratio is the same as the bound peptide/lipid ratio.

We found that while both peptides bind with high affinity to fluid lipid membranes, peptides were unable to penetrate into the membrane in the gel state. Fig. 1A shows the temperature dependence of the fluorescence energy transfer from peptide tryptophan to an anthrylvinyl fluorophore attached to the acyl chain of a phospholipid (APC). Fluorescence was excited at 295 nm (peptide) and measured at 435 nm (probe). Fluorescence intensity is dependent on the

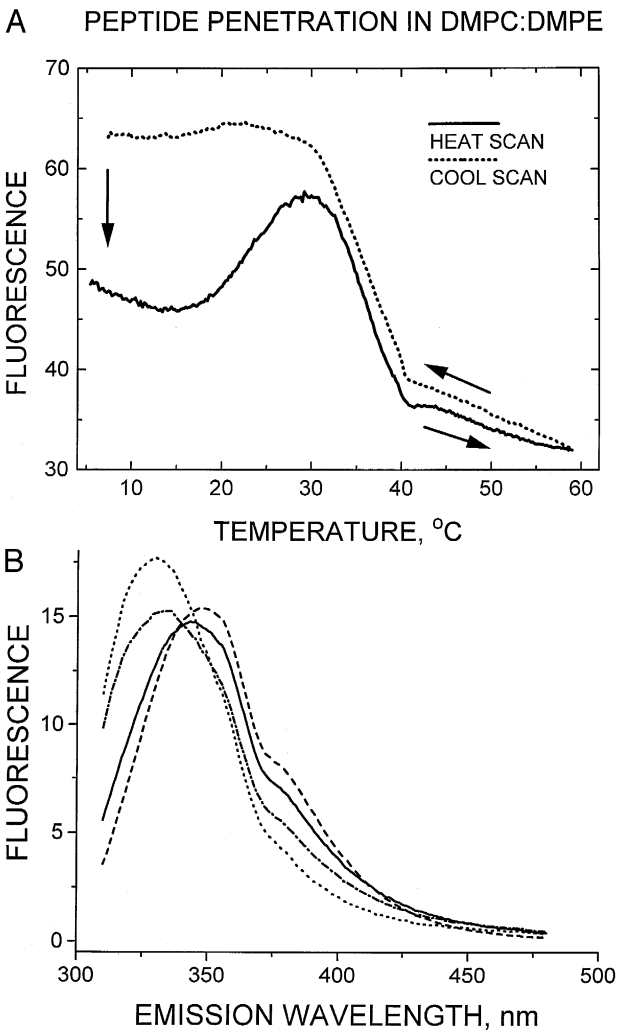

Fig. 1. A: temperature dependence of energy transfer from peptide to probe. Fluorescence was excited at 295 nm (peptide) and measured at 435 nm (anthrylvinyl probe (APC)). Ac-18A-NH_2 peptide (5 μM) was added at 6°C to gel state DMPC/DMPE (1:1) LUV (50 μM) labeled with 1% APC. The sample was heated up to 59°C. Increase in fluorescence at around 20–30°C is due to peptide insertion into the bilayer. The main phase transition is accompanied by a reversible decrease in the fluorescence intensity due to increased water permeability of the bilayer and temperature-dependent quenching of the probe. Upon cooling, the peptide is kinetically trapped in the gel phase. Fluorescence intensity returned to the initial values after overnight storage of the sample at 4°C. Both heating and cooling was at a constant rate of 0.5°C/min. B: tryptophan fluorescence of 18L (5 μM) in water (dashed line), after the addition of 50 μM of DMPC/DMPE (1:1) LUV at 8°C (solid line), after heating to 42°C (short-dashed line) and after cooling to 4°C (dash-dotted line). Spectrum of the sample stored overnight at 4°C was the same as after lipid addition (solid line). All spectra were scaled to the same integral intensity.

average distance between the peptide tryptophan and the fluorophore embedded in the bilayer. Ac-18A-NH_2 (1 mM) was added to DMPC/DMPE (1:1) MLV (10 mM) in the gel state at 6°C. The sample was heated to 59°C. An increase in fluorescence at around 20–30°C is due to peptide insertion into the bilayer at the beginning of gel phase melting. The main phase transition is accompanied by a reversible decrease in the fluorescence intensity. In control experiments (data not shown), peptide tryptophan fluorescence in unlabeled vesicles monotonously decreased with increasing temperature, but without abrupt changes in the region of the main phase transition. With the other control, labeled vesicles, but no peptide added, probe fluorescence decreased monotonicly with rising temperature and with a steeper slope in the region of the phase transition. The intensity of the emission from direct probe excitation was much lower than that due to the fluorescensce resonance energy transfer from peptide tryptophan. Taking into account the controls, we ascribe the reversible change in fluorescence around the main phase transition to increased temperature quenching of the probe and lateral expansion of the bilayer increasing the average distance between peptides and probes. Upon cooling, peptides stayed in the membrane; however, this peptide entrapment was kinetic, rather than thermodynamic, as peptides dissociated from the membranes on a time scale of hours. Fluorescence intensity returned to the initial values after overnight storage of the sample at 4°C. Decrease in energy transfer from peptide to probe can also be due to probe segregation into a separate phase. However, this should be accompanied by probe self-quenching, which was not observed.

Tryptophan fluorescence supports the energy transfer data. Addition of gel state liposomes to a peptide solution resulted in a limited blue shift of the tryptophan fluorescence. Melting the gel state results in a significant blue shift of the tryptophan fluorescence. Cooling below the main phase transition results in a small red shift, and subsequent overnight storage in the cold results in a further red shift of the spectra to one equivalent to that observed upon addition of gel state liposomes to peptide solution. An example of this sequence of events is illustrated for the case of the 18L peptide and DMPC/DMPE liposomes (Fig. 1B). In principle, the change in the position of tryptophan fluorescence maximum can be due to both an altered membrane bound state of the peptide or to an altered peptide partitioning between membrane and water. However, when corrected for the background, the position of tryptophan fluorescence maximum was constant over a wide range of lipid (20–500 μM) concentrations (data not shown). This is indicative that in this range of lipid concentrations, as with fluid membranes [12], 18L peptide was essentially all membrane bound. This means that the change in the position of maximum corresponds to an altered membrane-bound state, a change in the extent of peptide insertion into the membrane.

Metastability of peptide interactions with gel phase lipids had been reported previously [28,29]. Our data show that this metastability is observed even at low peptide/lipid ratios, not accompanied by vesicle disruption. Similar behavior was observed for both 18L and Ac-18A-NH_2 for several lipid systems (DMPC, DMPE, DMPC/DPPE) (data not shown). This suggests that such metastability may be a general feature of membrane–amphipathic peptide interactions. In single-component lipid systems, the main phase transition occurs over a narrower temperature range than in lipid mixtures. This was also reflected by the temperature dependence of peptide incorporation. The fluorescence increase coincides not with the completion, but rather was close to the onset, of the phase transition. This can be explained by taking into account the high affinity of 18L and Ac-18A-NH_2 peptides for membranes in the fluid phase [12] as well as the presence of phase boundary defects in the mixed phase region. The exact temperature at which incorporation is complete depended, as expected, on the peptide/lipid ratio and the peptide-fluid membrane binding constant.

3.2. Peptide effects on the lateral organization of the fluid phase

When the membrane consists of several molecular species, one can imagine that interaction of peptides with such a membrane occurs not with the membrane as a whole, but rather via association of peptides with particular lipid species. Geometric (Shape) factors were previously found to modulate many aspects of 18L and Ac-18A-NH_2 membrane interactions [11,12]. Correlation between the shape and the activities of

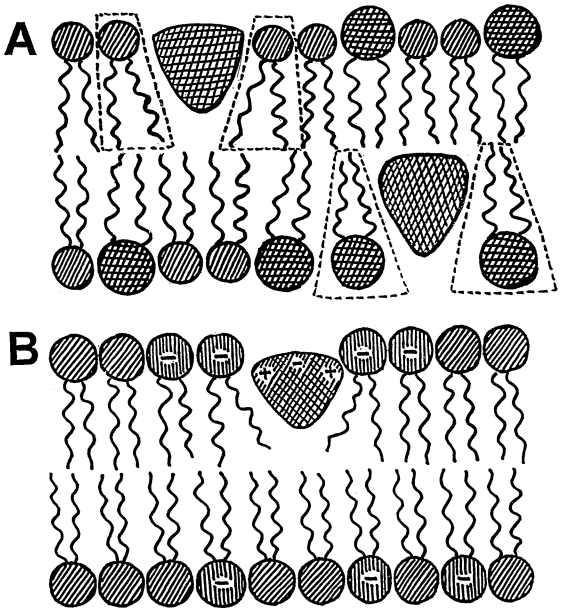

Fig. 2. Tentative mechanisms of peptide induced lateral lipid segregation. A: shape complementarity mechanism. Peptides are depicted in the projection along the axis of the α-helix. B: charge–charge interactions. Vicinity of cationic amino acid residues is suggested to be enriched with anionic lipids relative to the rest of the membrane.

peptides was especially pronounced for lipid systems with a propensity for non-bilayer phase formation, such as Me-DOPE/DOPC and DOPC/DOPE mixtures. Non-bilayer phase propensity is defined as the existence of high negative intrinsic monolayer curvature stress – a parameter defined for the membrane as a whole. In lipid mixtures where the possibility of lateral phase separation exists, there might exist a difference between the global and a local monolayer curvature. Thus a description only in terms of curvature stress, valid for single lipid systems, might be an oversimplification for lipid mixtures. We decided to test if the geometric shape of peptide molecules can induce lateral separation of membrane lipids. This hypothetical 'shape complementarity' mechanism of induction of lateral phase separation is illustrated in Fig. 2A. Another tentative motif for lateral phase organization is illustrated on Fig. 2B. Charge–charge interactions have been shown previously to affect 18L and Ac-18A-NH_2 membrane interactions [12] and it is natural to suppose that charge–charge interactions between acidic lipids and basic amino acid residues can lead to lateral separation of lipids. As an approach to the investigation of peptide-induced lateral organization of the membranes, we used energy transfer from membrane bound peptide tryptophan to the anthrylvinyl fluorophore of a lipid-specific probe. It was shown that deviation of the concentration dependence of energy transfer efficiency can be used as an indication of the non-random distribution of probe molecules [26]. It has been shown that distribution of anthrylvinyl-labeled lipid-specific probes in the plane of the membrane corresponds to that of their unlabeled counterparts [16,30]. Comparing the efficiency of resonance energy transfer for different types of lipid probes, one can detect preferential association of peptides with particular lipid species.

The DMPC/DMPG (1:1) mixture had been studied as an example of an acidic lipid-containing membrane. 18L is cationic and Ac-18A-NH_2 has positive charges at the peptide–lipid interface, although overall it is zwitterionic. For both peptides, the efficiency of transfer to APG was significantly higher than to

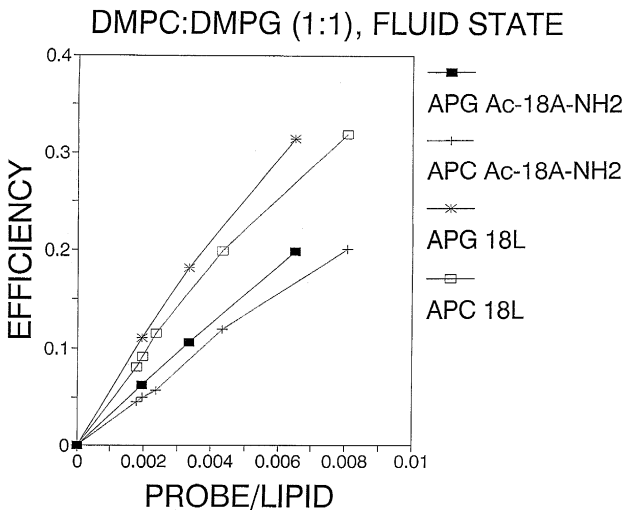

Fig. 3. DMPC/DMPG (1:1) LUV, fluid state (37°C), peptide/lipid molar ratio, 1:10. Dependence of the efficiency of peptide to probe fluorescence energy transfer on the molar fraction of probe in the membrane. ∗, 18L peptide, membranes labeled with APG; □, 18L peptide, membranes labeled with APC; ■, Ac-18A-NH_2 peptide, membranes labeled with APG; +, Ac-18A-NH_2 peptide, membranes labeled with APC. FRET efficiency is calculated as described in Section 2: Materials and methods. Experimental errors are within the size of the symbols. Higher efficiency of energy transfer to the APG probe is indicative of the preferential association of both types of peptides with acidic lipids. Higher efficiencies observed for 18L are indicative of its deeper penetration into the bilayer.

APC, which is an indication of the preferential association of both peptides with acidic lipids (Fig. 3). Significant differences in the efficiency of energy transfer were also observed between Ac-18A-NH_2 and 18L, which we can attribute to the increased depth of incorporation of 18L into membranes. Originally, peptides were added to the fluid membrane. If cooled down below phase transition, these peptides remained kinetically trapped in the membrane. Energy transfer in the gel phase was larger than in the fluid state and the difference between two types of peptides and two types of probes was more pronounced than in the fluid phase (not shown).

We supposed that peptides might induce lateral lipid separation in the DOPC/DOPE (1:1) system as a consequence of a shape compensation mechanism. However, coincidence of the efficiencies of transfer from peptide to APC or APE is indicative of complete mixing in this system (Fig. 4). Coincidence of the curves measured for two types of peptides indicates the similar depth of penetration of peptide tryptophan into the bilayer. This was also supported by the coincidence of tryptophan fluorescence spectra of both peptides associated with DOPC/DOPE (1:1) membranes (not shown). Since we have seen no evidence of preferential association of peptides with lipids according to a shape compensation mechanism, we conclude that effects of peptides on this membrane are mediated via modulation of the physical properties of the membrane as a whole, rather than via membrane domain formation. A similar picture of the complete coincidence of energy transfer dependencies between APC or APE and 18L or Ac-18A-NH_2 was also observed with DMPC/DMPE (data not shown).

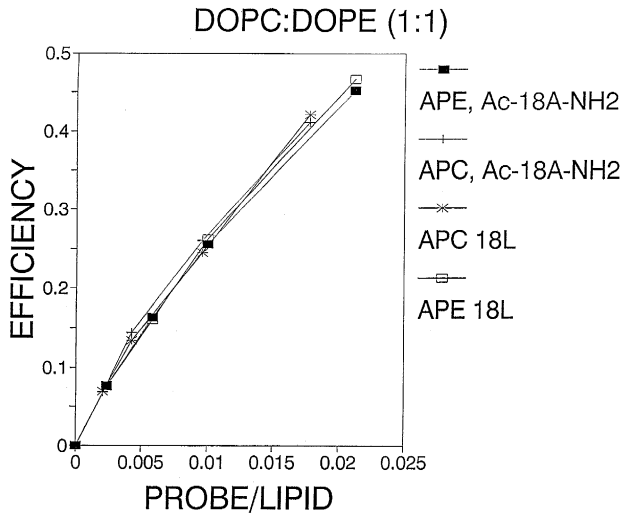

Fig. 4. DOPC/DOPE (1:1) LUV, peptide/lipid ratio, 1:10. Dependence of the efficiency of fluorescence peptide to probe energy transfer on the molar fraction of probe in the membrane. ∗, 18L peptide membranes labeled with APC; □, 18L peptide, membranes labeled with APC; ■, Ac-18A-NH_2 peptide, membranes labeled with APE; +, Ac-18A-NH_2 peptide, membranes labeled with APC. FRET efficiency is calculated as described in Section 2: Materials and methods. Experimental errors are within the size of the symbols. Coincidence of the efficiencies of transfer from peptide to APC or APE is indicative of the complete mixing in the system. Coincidence of the curves measured for two types of peptides indicates the similar depth of penetration of peptide tryptophan into the bilayer.

To estimate the extent of demixing of lipid species in the presence of peptides, we used fluorescence energy transfer from anthrylvinyl-labeled to perylenoyl-labeled phospholipid probes. Efficiency of energy transfer is dependent on the average distance between donor and acceptor and thus is sensitive to deviations from a random distribution of probes. We titrated DOPC/DOPG (1:1) membranes, containing either APC/PPC or APG/PPC donor/acceptor pairs, with peptides and monitored the change in energy transfer efficiencies in these systems (Fig. 5A). We found that for both peptides, the relative decrease of transfer efficiency was the same for both pairs. Transfer efficiency is primarily sensitive to the surface density of acceptor (PPC in this case), which was the same for both donor/acceptor pairs. However, transfer efficiency will be differently affected by separation or accumulation of either donor or acceptor in domains having sizes larger than the Foerster radius (R_o) for this donor/acceptor pair. Thus the coincidence of the relative decrease in intensity suggests that there does not occur lateral separation on a scale larger than R_o, which is on the order of 44 Å for the anthrylvinyl/perylenoyl donor/acceptor pair [31]. A decrease in energy transfer efficiency between two lipid probes upon increasing of membrane peptide content can be used to estimate the surface occupied by one membrane-inserted peptide molecule (see Section 2 Materials and methods). The relative decrease in transfer efficiency is plotted against the peptide/lipid ratio (Fig. 5A). This gives the ratio of the surfaces occupied by one peptide vs. one lipid molecule. Both the APC/PPC

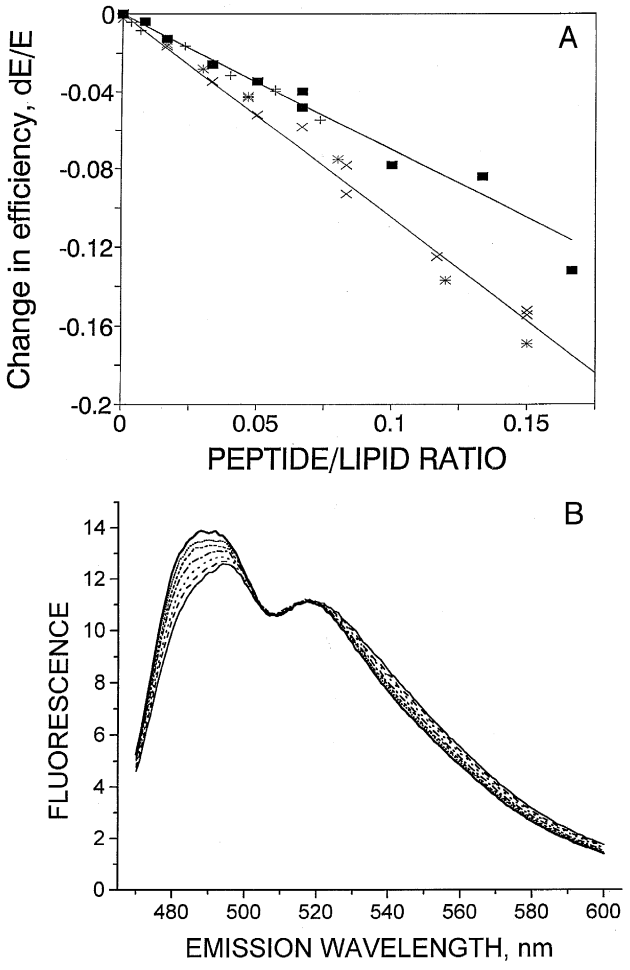

Fig. 5. A: changes in the efficiency of the fluorescence energy transfer from APC (2%) to PPC (1%) and from APG (2%) to PPC (1%) upon titration of DOPC/DOPG (1:1) LUV with amphipathic peptides. Decrease in efficiency is due to an increase in surface area of the bilayer upon peptide insertion. Titration with 18L: ■, APC/PPC donor/acceptor pair; +, APG/PPC pair. Titration with Ac-18A-NH_2: ∗, APC/PPC donor/acceptor pair; ×, APG/PPC pair. Straight lines were derived by linear regression, separately for 18L and for Ac-18A-NH_2. B: changes in the shape of PPC fluorescence spectra in the process of titration of DOPC/DOPG (1:1) LUV with Ac-18A-NH_2 peptide. Curves correspond to the following peptide/lipid ratios: solid, 0; dashed, 1/60; dotted, 1/30; dash-dotted, 1/20; short-dashed, 1/15; short-dotted, 1/12; heavy solid, 1/6.7. These spectral changes correspond to a decrease in polarity of the fluorophore environment.

and the APG/PPC donor/acceptor pairs report a surface occupied by 18L, $S_{18L} = 0.7 \times S_l$ and by Ac-18A-NH_2, $S_{Ac\text{-}18A\text{-}NH2} = 1.05 \times S_l$ where S_l is the average surface per lipid molecule in this DOPC/DOPG (1:1) membrane. Values of 70 ± 4 Å^2/lipid have been reported for DOPC in the L_α phase [27]. There are no available data on the average surface per molecule in a DOPG or a DOPC/DOPG (1:1) membrane. However, it is a reasonable estimate that the surface per lipid molecule in DOPC/DOPG (1:1) is close to 70 Å^2, since the surface area of various phosphatidylglycerols parallels their phosphatidylcholine analogs [40].

An interesting related observation is that for both 18L and Ac-18A-NH_2, upon an increase of peptide content in the membrane, changes in PPC fluorescence spectra indicated a decrease in the polarity of the environment of PPC. This is similar to the finding that had been previously [18] interpreted as a decrease of water permeability and/or water content of the bilayer. Changes in PPC spectra upon addition of Ac-18A-NH_2 to DOPC/DOPG 1:1 LUV are shown in Fig. 5B.

3.3. Peptide effects on the existing phase separation (gel–liquid crystal)

We found that preferential association of peptides with acidic lipids was capable of modulating a preexisting lateral organization of the membrane, that is, in the course of the gel–liquid crystalline phase transition both peptides stabilized or destabilized the gel phase, depending on whether acidic lipids (PG) were the low or the high melting component (Fig. 6). Anisotropy of fluorescence of the C_{12} - attached anthrylvinyl fluorophore has long been known to be sensitive to the phase state of the surrounding lipid [15,16]. PC/PG vesicles labeled with APC or APG probes have been prepared. PC/PG systems are often regarded as systems with almost ideal mixing. Thus phase transitions as reported by both APC and APG probes are essentially coincident. There was only a minor shift between cooling and heating scans. Addition of peptide similarly changed the temperature dependencies of the fluorescence anisotropy reported by both probes, APC and APG. Ac-18A-NH_2 addition is shown in Fig. 6. Similar effects were observed upon addition of 18L (data not shown). These findings suggest that peptide association with acidic lipids does not cause complete lateral separation of PC and PG.

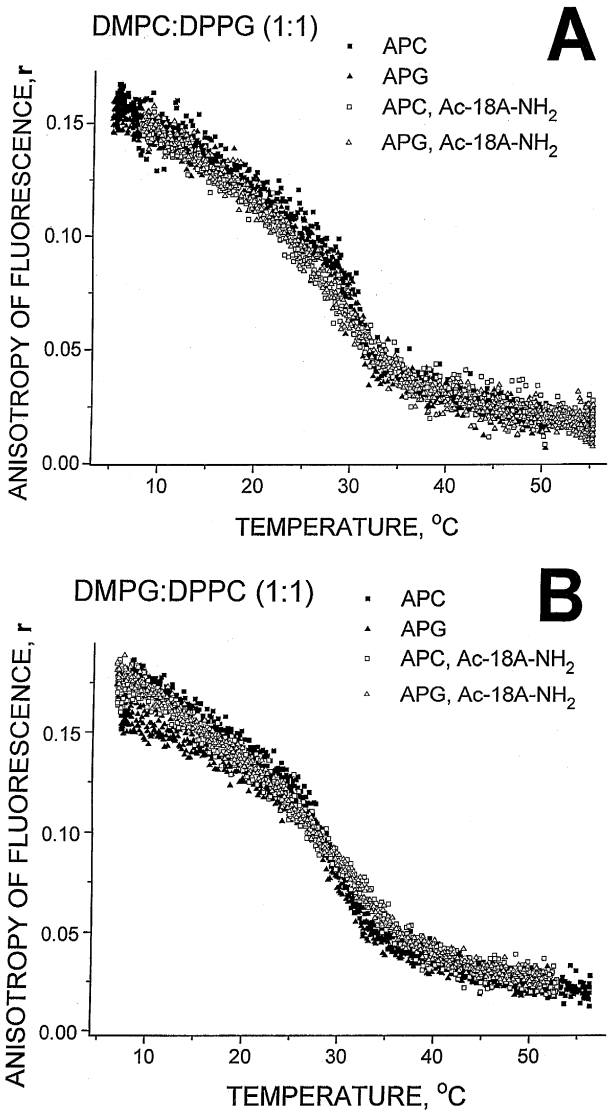

Fig. 6. Temperature dependencies of the anisotropy of fluorescence of probes APC and APG in PC/PG MLV in pure lipid membranes and in the presence of Ac-18A-NH_2 (peptide/lipid molar ratio, 1:10). Before the data acquisition, vesicles were cycled through the main phase transition and then kept for 30 min in the cold. Heating scans are shown. Vesicles were labeled with 0.2 molar % of corresponding probes. A: DMPC/DPPG (1:1). ■, vesicles labeled with APC; □, vesicles labeled with APC in the presence of Ac-18A-NH_2; ▲, vesicles labeled with APG; △, vesicles labeled with APG in the presence of Ac-18A-NH_2. B: DMPG/DPPC (1:1). ■, vesicles labeled with APC; □, vesicles labeled with APC in the presence of Ac-18A-NH_2; ▲, vesicles labeled with APG; △, vesicles labeled with APG in the presence of Ac-18A-NH_2.

In the case when acidic lipids were the low temperature melting component (DMPG/DPPC, Fig. 6B), in the absence of peptide, both APC and APG probes (closed symbols) reported a phase transition at 24.5–33°C. Addition of peptide broadened the transition to about 24–36°C. This pronounced upshift of the temperature of completion of the phase transition, can be explained as a result of the depletion of gel phase from acidic lipids due to charge–charge peptide–lipid interactions. Gel phase depleted of the low melting component thus has the higher melting temperature.

In the case when acidic lipids were the higher melting component (DMPC/DPPG, Fig. 6A) peptide addition also broadened the phase transition from about 30–32.5°C to 27–33°C. The more pronounced here was the downshift of the temperature of the onset of the phase transition. The anisotropy of both probes was lower in the presence of either peptide through most of the main phase transition than in the lipid only membranes. This illustrates that preferential association of peptides with acidic lipids can decrease the stability of the gel phase. Naturally, peptide insertion in the membrane at relatively high peptide/lipid ratios (1:10, as in Fig. 6) is likely to disrupt the stability of the gel phase, even without any specific lateral peptide–lipid association. Peptides also induced a downshift and broadening of the main phase transition in pure lipid systems (DMPC or DMPG, not shown) or when lipids had similar phase transition temperatures (DMPC/DMPG, not shown), but quantitatively the shift was less pronounced.

We also studied peptide effects on the main phase transition in zwitterionic membranes known for non-ideal lipid mixing (DMPC/DMPE, DMPC/DPPE) [16,33,34]. A large hysteresis between heating and cooling scans had been observed in this system (not shown). In the absence of peptides in this system, APC and APE probes report the phase transition differently, with a shift of both the onset and completion temperatures (Fig. 7, closed symbols). These differences in anisotropy corresponds to markedly different probe environments through the whole temperature range of the phase transition, suggesting the existence of some sort of lateral organization in the plane of the bilayer, enrichment of fluid domains with PC and gel with PE. Upon addition of peptide

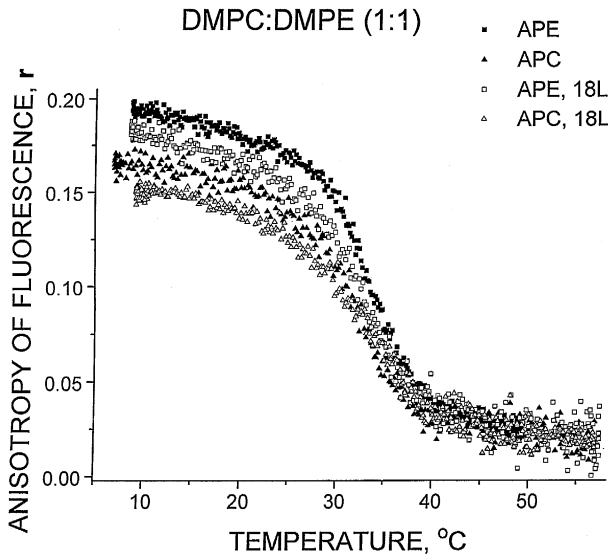

Fig. 7. Temperature dependencies of the anisotropy of fluorescence of probes APE and APC in DMPC/DMPE (1:1) MLV in pure lipid membranes and in the presence 18L (peptide/lipid molar ratio, 1:10). Heat scans are shown. ■, vesicles labeled with APE (0.2 molar %); □, vesicles labeled with APE (0.2 molar %) in the presence of 18L; ▲, vesicles labeled with APC (0.2 molar %); △, vesicles labeled with APC (0.2 molar %) in the presence of 18L.

(18L–DMPC/DMPE, 1:10, Fig. 7, open symbols) the anisotropy of the fluorescence of APC and APE coincided in the mid-transition range. Anisotropy of APE decreased while that of APC increased, suggesting that the probe environments changed from being distinctly different to being rather similar. Such a change may be interpreted as an increase in the miscibility of this system. This may not be as much a change of domain composition as a reduction of the domain size, so that the anisotropy is more averaged throughout the membrane. Another indication on the increase of miscibility in this system is the reduction of hysteresis between heating and cooling scans in the presence of peptide. Addition of peptide (18L on Fig. 7, Ac-18A-NH_2, not shown) also broadens the phase transition and decreases the anisotropy values in the gel phase.

We tried to detect peptide-induced changes in APC and APE fluorescence anisotropy directly by the peptide titration experiments; however, the resolution was found to be insufficient. There was a principal problem of peptide equilibration between layers of MLV at constant temperature, as well as interference with other peptide-induced effects like membrane fusion and vesicle aggregation. In addition, the anisotropy in the range of the phase transition is susceptible to large fluctuations and thus is strongly dependent on the history of the sample. We also made temperature scanning experiments with peptide/lipid ratios other than 1:10. The results were qualitatively the same. Further increase in peptide content resulted in further shifts in transition temperatures and was accompanied by further broadening of the transitions. With a reduction of peptide content, anisotropy scans were more like those for the pure lipid systems.

Besides anisotropy, as an approach to study the temperature dependence of peptide effects on membrane lateral organization, we used fluorescence energy transfer from APC or APG to PPC. The complexity of this approach is that the fluorescence properties of probes are temperature dependent and this dependence is also related to the phase state of the membrane. Thus external standards, such as dilution with detergent are not so useful. Calculation of energy transfer efficiency in this approach is also more approximate because instead of deconvoluting spectra, we only measured intensity at two particular wavelengths, corresponding to anthryl (435 nm) and perylenoyl (510 nm) fluorescence. We neglect the dependence of quantum yield of perylenoyl fluorescence on temperature and medium polarity, which is not strictly correct. To get an insight into the molecular organization of the membranes, we suggest comparing the temperature dependencies of FRET efficiencies in the presence and in the absence of peptides. In DMPC/DMPG (1:1) vesicles, in the absence of peptides, the temperature dependencies of FRET efficiencies were similar for APC/PPC and APG/PPC donor/acceptor pairs (Fig. 8). However, 18L (Fig. 8) addition changed these dependencies in opposite ways. Upon heating without peptide, the efficiency was increasing several degrees below the main phase transition and decreasing with the onset of the phase transition. This decrease was essentially complete before the completion of the phase transition. After melting, the efficiency decreased slowly over a wide range of temperatures. There was very little hysteresis in this system, heating and cooling scans were nearly superimposable (only heating scans are shown in Fig. 8). In the fluid phase, addition of 18L (Fig. 8) decreased transfer efficiency due to the

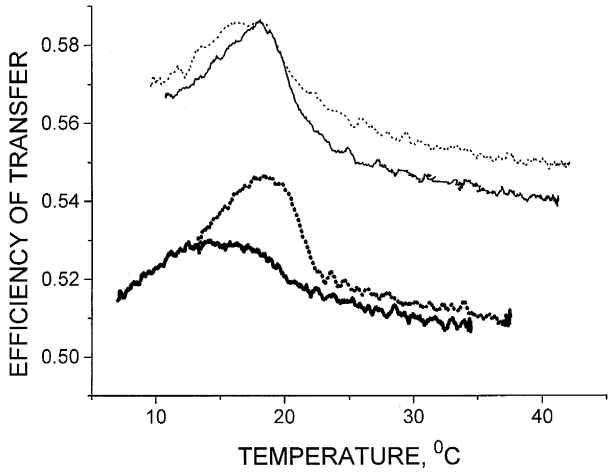

Fig. 8. Temperature dependencies of the efficiency of the fluorescence energy transfer between two types of lipid specific fluorescent probes (APC (2 molar %) to PPC (1 molar %) (dotted lines) or APG (2 molar %) to PPC (1 molar %) (solid lines)) in the course of the main phase transition of DMPC/DMPG (1:1) LUV, lipid only systems (thin lines) or with molar 5% of 18L (bold lines). Heating scans are shown.

increase in the surface area upon peptide incorporation, in accordance with Fig. 5A. However, increase in transfer efficiency below the lipid phase transition was smoothed out for APC/PPC, while it was enhanced for APG/PPC. The temperature of maximum energy transfer also shifted in different directions: from 17 to 18.5°C for APG/PPC, and from 18 to 16°C for APC/PPC. The difference between heating and cooling scans became more pronounced for APG/PPC, although it was shifted only 1°C. Similar changes were observed for the addition of Ac-18A-NH_2 (not shown). These data are in agreement with anisotropy experiments (Fig. 6A), which suggest that in this system peptide serves as a nucleation site for gel phase melting, and also with peptide-to-probe FRET experiments (Fig. 3) which suggest that the peptide environment is enriched in acidic lipids. Previously, we found that the PPC probe has some preference for the fluid phase [16]. Thus, the beginning of membrane melting in the presence of peptide, for the APG/PPC pair, results in the increased accumulation of both probes in the fluid phase (peptide vicinity) and consequently in the increase of energy transfer, relative to that in the absence of peptide. Contrary to that, peptide domain formation and PPC preference for the fluid phase will contribute to the demixing of donor and acceptor for the APC/PPC pair and thus will result in smoothing of the temperature dependence of energy transfer efficiency.

4. Discussion

Several fluorescence approaches were used to show that amphipathic peptides can induce lateral lipid separation in membranes as well as modulate existing lateral organization. Fluorescence detection is very sensitive to domain formation in the sense that the minimum domain lifetime to be detected is about the lifetime of the fluorophore excited state, i.e., on the scale of 10^{-8} s. Spacial resolution is about equal to the Foerster radius, i.e., 24 Å for the Trp/anthrylvinyl pair and 44 Å for the AV/perylenoyl pair. This means that the fluorescence method is sensitive to everything from membrane dynamic heterogeneity to stable domain formation on the scale of parts of the whole cell, although discrimination among the possibilities would require imaging methods.

One can imagine three types of lateral organization: segregated, random and regular. In binary lipid mixtures, this approximately corresponds to preferences in like–like interactions, absence of preference, or preference of dislike interactions. Naturally, situations intermediate between these extremes are of biological relevance. Discussion of lateral organization in PE/PC systems usually centers around the possibility of segregation due to like–like association via the intermolecular hydrogen bond formation between PE headgroups. In the fluid phase of PE/PC mixtures we did not observe any evidence of this type of association. Our data also rule out any heterogeneity in DOPC/DOPE and DMPC/DMPE (in L_α phase) mixtures in the presence of peptides. The effects of L- and A-type amphipathic peptides on biological membranes and on model membranes with propensity for non-bilayer phase formation had been shown to correlate with the peptide modulation of intrinsic monolayer curvature (IMC) of the membrane [11,12]. Application of the IMC concept to a multi-component system has to deal with the possible difference between short range order (local) and long range order (global), due to lateral lipid domain formation. Our data on the complete lipid miscibility show that a description in terms of global IMC can

be applied, not only for single-component systems (like Me-DOPE), but also for binary and possibly multi-component zwitterionic membranes.

Contrary to the case of zwitterionic PC:PE systems, in anionic PC/PG membranes both Ac-18A-NH_2 and 18L peptides affected membrane lateral organization. PC/PG membranes with identical or similar hydrophobic chains are usually discussed in terms of complete mixing [35,36] or regular lateral organization [37]. It should be noted that macroscopic methods, like DSC, often used for analysis of lipid phase behavior, do not easily discriminate between these two types of organization [3]. Electrostatic repulsion between anionic PG headgroups is a natural reason why these membranes may have a motif of regular lateral membrane organization. Both Ac-18A-NH_2 and 18L have basic residues (lysines). In the membrane associated state, electrostatic interactions of peptide lysines with anionic lipids would result in the accumulation of acidic lipids in the vicinity of the peptide. The size of these domains enriched in acidic lipids is not larger than the Foerster radius for the anthrylvinyl/perylenoyl donor/acceptor pair, as we had not seen significant lipid demixing in peptide titration experiments. Enrichment of the vicinity of the peptide with acidic lipids can be estimated from the data in Fig. 3. The efficiency of FRET from tryptophan to APL is primarily dependent on the surface density of APL in the vicinity of the peptide molecules, namely within R_o (~ 24 Å) distance around the peptide tryptophan. $E \approx \sigma_{local}$, is different from σ_o in the absence of peptide. As long as APL follows the distribution of the host PL, $\sigma_{local} = \sigma_o \cdot c_l/c_o$ where c_l is the concentration of host lipid in the vicinity of the peptide and c_o is the host lipid concentration in the absence of peptide. From this, we can conclude that the ratio of the FRET efficiencies derived by different probes directly corresponds to the ratio of two types of host lipids in the vicinity of the peptide: $E_{APC}/E_{APG} = (c_{l,PC}/c_{o,PC})/(c_{l,PG}/c_{o,PG}) = c_{l,PC}/c_{l,PG}$ since $c_{oPC} = c_{oPG}$ in this DMPC/DMPG (1:1) system. Comparing the slopes of $E(\sigma)$ dependencies (Fig. 3) we get $c_{l,PC}/c_{l,PG} =$ 0.75 for Ac-18A-NH_2 and 0.7 for 18L. This estimate is only a minimum for the case in which the actual domain arrangement is restricted to an area less than the Foerster radius, that is, if the actual organization is close to the stoichiometric association of acidic lipids with cationic residues of the peptide. Indication that peptide effects are pronounced at larger distances comes from data on bilayer expansion upon peptide insertion. In this case, relatively low enrichment of acidic lipids suggests the dynamic character of this lateral domain structure.

Low values of bilayer surface expansion upon peptide insertion are indicative that peptide insertion is accompanied by more dense packing of the bilayer. In the absence of peptides, besides just steric considerations, charge–charge repulsions between charged lipid molecules affect the surface area per molecule. Insertion of the peptide reduces lipid–lipid repulsion in the vicinity of the peptide and thus reduces the surface area per lipid molecule around the peptide. This results in apparent reduction of the measured surface occupied by one peptide molecule. More dense packing of the bilayer is also reflected in the spectra of the perylenoyl probe which corresponds to a less polar environment (Fig. 5B). Huang et al., recently reported that membrane insertion of amphipathic peptides magainin 2 and alamethicin leads to bilayer thinning [38,39]. This effect, was suggested to be general for side inserting amphipathic peptides. If we assume that it is pronounced for the peptides we studied here, then bilayer thinning, taken together with only a small surface increase upon peptide insertion, will mean a reduction in membrane hydrophobic volume and thus an increase in the packing density in the hydrophobic part of the bilayer.

The larger surface increase by Ac-18A-NH_2 is predictable since its hydrophilic surface is larger than that of 18L; there are 8 charged residues in this peptide compared with 4 in 18L. Also, the zwitterionic peptide Ac-18A-NH_2 is less potent than cationic 18L in screening anionic lipids. The small surface area occupied by the peptide also confirms the 'snorkel hypothesis' of Mishra et al. [41] that the long hydrophobic part of the lysine side chain contributes to the insertion of the peptide.

Creation of domains is entropically unfavorable. Strong interactions, such as charge–charge interactions are required to cause preferential peptide–lipid association. More pronounced peptide effects are observed around the main phase transition of the bilayer, a state which is intrinsically susceptible to large fluctuations because phase coexistence results in less ordered packing of the lipids. Generally, pep-

tide insertion reduces the cooperativity of the phase transition. However, in other respects peptide effects are dependent on the lipid system. In zwitterionic PC/PE systems, known for non-ideality of mixing, peptide addition reduces the difference in the PC and PE probe's environments (Fig. 7), that is, the peptide increases mixing in these systems. Peptide preference for the fluid phase is expected since peptides cannot stably incorporate into the gel phase (Fig. 1). Along with this general fluid phase preference, peptide–lipid charge–charge interactions affected lateral membrane organization in the course of the main phase transition. When acidic lipids were the low melting component of the lipid mixture, peptide–acidic lipid interactions resulted in the depletion of the low melting component from the gel phase and thus shifting the completion of the phase transition to the higher temperatures. When acidic lipids were the high melting component of the binary mixture, peptide addition resulted in the broadening and shifting to lower temperatures of the onset and T_m of the transition. Contrary to the PC/PE system, in the PC/PG systems anisotropy values of the APC and APG probes essentially coincided, and there was only a very small difference between heating and cooling scans. This also indicates a high miscibility in this system. While peptide affected the phase transition in these systems, there was no detectable difference between the anisotropy measured by APC and by APG. This also indicates the nanoscopic scale of lateral organization, that is, there were no separated domains big enough to maintain different motional order.

Despite belonging to different classes of amphipathic helices and opposing activities on biological or model zwitterionic membranes, both 18L and Ac-18A-NH_2 peptides have similar effects on membrane lateral organization. The difference between peptide effects was quantitative rather than qualitative, for example, Ac-18A-NH_2 has a 50% larger surface increase upon membrane incorporation than 18L. The similarity of the effects of 18L and Ac-18A-NH_2 peptides on membranes lateral organization suggests the general character of the observed patterns. Charge–charge peptide–lipid interactions are capable of modulating lateral membrane organization both in the fluid state and in the course of the main phase transition. Contrary to electrostatic interactions, the geometrical factors, the shape of peptide molecule, were unable to induce demixing of lipid components of fluid membranes. Peptides of different shape were found to increase lipid mixing similarly in membranes known for mixing non-ideality (DMPC/DMPE). The absence of complex peptide-induced lateral organization in fluid zwitterionic lipid mixtures supports the validity of a description of peptide–membrane interactions in terms of affecting parameters of the membrane as a whole, such as intrinsic monolayer curvature modulation.

Acknowledgements

We would like to thank Dr. G.M. Anantharamaiah and Dr. J.P. Segrest for provided peptides and for advice on the manuscript. The work had been supported by the Medical Research Council of Canada Grant MT-7654.

References

[1] L.D. Bergelson, K. Gawrisch, J.A. Ferretti, R. Blumenthal (Eds.), Special issue on Domain Organization in Biological Membranes, Mol. Mem. Biol. 12 (1995) 1–162.
[2] R. Welti, M. Glaser, Chem. Phys. Lipids 73 (1994) 121–137.
[3] A. Raudino, Adv. Coll. Inter. Sci. 57 (1995) 229–285.
[4] K. Jacobsen, W.L.C. Vaz (Eds.), Topical Issue on Domains in Biological Membranes, Commun. Mol. Cell. Biophys. 8 (1992) 1–114.
[5] O.G. Mouritsen, K. Jorgensen, Chem. Phys. Lipids 73 (1994) 3–25.
[6] P. Luan, L. Yang, M. Glaser, Biochemistry 34 (1995) 9874–9883.
[7] J.H. Davis, M. Bloom, D.M. Clare, R.S. Hodges, Biochemistry 22 (1983) 5298–5305.
[8] O.G. Mouritsen, M. Bloom, Annu. Rev. Biophys. Biomol. Struct. 22 (1993) 145–171.
[9] R.M. Epand (Ed.), The Amphipathic Helix, CRC Press, Boca Raton, FL, 1993.
[10] J.P. Segrest, H. De Loof, J.G. Dohlman, C.G. Brouillette, G.M. Anantharamaiah, Proteins 8 (1990) 103–117.
[11] E.M. Tytler, J.P. Segrest, R.M. Epand, S.Q. Nie, R.F. Epand, V.K. Mishra, Y.V. Venkatachalapathi, G.M. Anantharamaiah, J. Biol. Chem. 268 (1993) 22112–22118.
[12] I.V. Polozov, A.I. Polozova, E.M. Tytler, G.M. Anantharamaiah, J.P. Segrest, G.A. Woolley, R.M. Epand, Biochemistry, in press.
[13] Y.V. Venkatachalapathi, M.C. Phillips, R.M. Epand, R.F. Epand, E.M. Tytler, J.P. Segrest, G.M. Anantharamaiah, Proteins 15 (1993) 349–359.

[14] F. Paltauf, H.H.O. Schmid (Eds.), Special issue, Fluorescence in Membrane Biochemistry, Chem. Phys. Lipids 50 (1989) 171–289.
[15] L.D. Bergelson, J.G. Molotkovsky, Y.M. Manevich, Chem. Phys. Lipids 37 (1985) 165–193.
[16] I.V. Polozov, J.G. Molotkovsky, L.D. Bergelson, Chem. Phys. Lipids 69 (1994) 209–218.
[17] J.G. Molotkovsky, V.I. Babak, L.D. Bergelson, Y.M. Manevich, Biochim. Biophys. Acta 778 (1984) 281–288.
[18] J.G. Molotkovsky, L.D. Bergelson, M.O. Karyukhina, Biol. Membr. 4 (1987) 387–394.
[19] J.G. Molotkovsky, P.I. Dmitriev, L.F. Nikulina, L.D. Bergelson, Bioorgan. Khim. 5 (1979) 588–594.
[20] J.G. Molotkovsky, V.I. Unkovsky, L.D. Bergelson, Bioorgan. Khim. 6 (1980) 144–145.
[21] J.G. Molotkovsky, L.D. Bergelson, Bioorgan. Khim. 8 (1982) 1256–1262.
[22] J.G. Molotkovsky, L.D. Bergelson, M.O. Karyukhina, M.M. Smirnova, Bioorgan. Khim. 15 (1989) 686–689.
[23] B.N. Ames, Methods Enzymol. 8 (1966) 115–118.
[24] J.R. Lakowicz, Principles of Fluorescence Spectroscopy, Plenum Press, New York, NY, 1983.
[25] L.B.A. Johansson, J.G. Molotkovsky, L.D. Bergelson, Chem. Phys. Lipids 53 (1990) 185–189.
[26] B.K. Fung, L. Stryer, Biochemistry 17 (1978) 5241–5248.
[27] S.M. Gruner, M.W. Tate, G.L. Kirk, P.T.C. So, D.C. Turner, D.T. Keane, C.P.S. Tilcock, P.R. Cullis, Biochemistry 27 (1988) 2853–2866.
[28] R.M. Epand, Biochim. Biophys. Acta 514 (1978) 185–197.
[29] R.M. Epand, Biochim. Biophys. Acta 712 (1982) 146–151.
[30] I.A. Gromova, J.G. Molotkovsky, L.D. Bergelson, Chem. Phys. Lipids 60 (1992) 235–246.
[31] O.N. Smirnov, A.M. Surin, E.I. Astashkin, I.L. Mikhalyov, J.G. Molotkovsky, Biol. Membr. 12 (1995) 174–184.
[32] L.D. Bergelson, E.M. Manevich, J.G. Molotkovsky, G.I. Muzya, M.A. Martynova, Biochim. Biophys. Acta 921 (1987) 182–190.
[33] A.G. Lee, Biochim. Biophys. Acta 413 (1975) 11–23.
[34] E.J. Luna, H.M. McConnell, Biochim. Biophys. Acta 509 (1978) 462–473.
[35] E.J. Findlay, P.G. Barton, Biochemistry 17 (1978) 2400–2405.
[36] P.W. Van Dijck, B. De Kruijff, A.J. Verkleij, L.L. Van Deenen, J. de Gier, Biochim. Biophys. Acta 512 (1978) 84–96.
[37] J. De Bony, J.F. Tocanne, Eur. J. Biochem. 143 (1984) 373–379.
[38] S. Ludtke, K. He, H. Huang, Biochemistry 34 (1995) 16764–16769.
[39] Y. Wu, K. He, S.J. Ludtke, H.W. Huang, Biophys. J. 68 (1995) 2361–2369.
[40] D. Marsh, CRC Handbook of Lipid Bilayers, CRC Press, Boca Raton, FL, 1990.
[41] V.K. Mishra, M.N. Palgunachari, J.P. Segrest, G.M. Anantharamaiah, J. Biol. Chem. 269 (1994) 7185–7191.